Flow-injection Amperometry at Microfabricated Silicon-based μ-Liquid | Liquid Interface Arrays

Micheál D. Scanlon, Alfonso Berduque, Jörg Strutwolf, Damien W.M. Arrigan[1],[2],*

Tyndall National Institute, Lee Maltings, Univerisity College Cork, Ireland.

*Corresponding author: d.arrigan@curtin.edu.au

Fax: +61-(0)8-92664699

Abstract

Geometrically regular silicon membrane–based micropore arrays were employed for defined arrays of micrometer-sized interfaces between two immiscible electrolyte solutions (μITIES). These were incorporated into a poly(tetrafluoroethylene) (PTFE) hydrodynamic cell. Electrochemistry at the μITIES array was undertaken following gellification of the organic phase using polyvinyl chloride (PVC) and flowing an aqueous phase over the array surface. Cyclic voltammetric characterisation of asymmetric diffusion profiles on either side of the μITIES was accomplished under flowing conditions using positively and negatively charged (TEA^+ and 4-$OBSA^-$, respectively) model analyte species. Incorporation of an ionophore (dibenzo-18-crown-6 ether) into the organogel allowed the ion transfer detection of two oligopeptides (phenylalanine dipeptide and lysine dipeptide) within the available potential window under stationary and flowing conditions. Flow rate studies with TEA^+ indicated that the amperometric peak currents do not obey the Levich equation, due to diffusion dominating the mass transport, as opposed to convection. The influence of the applied potential ($\Delta_O^W\phi$) on the amperometric response of the oligopeptides was studied and hydrodynamic

[1] Member of ISE.
[2] Present Address: Nanochemistry Research Institute, Department of Chemistry, Curtin University of Technology, GPO Box U1987, Perth,WA 6845, Australia.

voltammograms (HDVs) for the individual oligopeptides were subsequently constructed. The data presented provide a basis for the use of silicon membrane-based μITIES arrays in flow analytical methods.

Keywords

Flow Injection Analysis, Amperometry, Micropores, Liquid | Liquid Interface, Oligopeptides, Hydrodynamic Voltammogram

1. Introduction

Inducing the transfer of ions across the interface between two immiscible electrolyte solutions (ITIES) by generating a potential difference between the two phases provides a powerful avenue for the detection of non-redox active species [1-11]. Flow injection analysis (FIA) of numerous charged species using a variety of electrochemical detection techniques (e.g. amperometric, voltammetric or chronocoulometric methods) has been reported at the liquid | liquid interface [12-33].

For analytical applications of such flow systems, the mechanical instability of the liquid | liquid interface was a problem addressed in a variety of ways. On the whole, this problem was circumvented by gellification of the organic phase with poly(vinyl) chloride (PVC) [12, 14, 18, 20, 24, 28-33] or insertion of solid porous membrane materials between the two immiscible solutions [13, 15-17, 21, 23, 25-27]. Inevitable reductions in diffusion coefficients of the analyte ions, associated with gellification of the organic phase, have not proven problematic when monitoring ion transfer by amperometric and voltammetric methods. Increases in uncompensated resistance in the cell due to gellification have been off-set by incorporating micropore or microhole arrays into the experimental setup [11, 19, 22]. Micrometre-sized ITIES (μITIES) play the dual role of integrating the advantages associated

with solid – state microelectrode arrays (reduced ohmic resistance, increased mass transport and sensitivities) into the system while also serving to provide mechanical stability. Recently we discussed the influence of the number of pores and the pore radius on the trans-membrane resistance of the solid-state membranes used in the present paper [34]. The iR-drop has a negligible effect on the transient currents at the gellified organic | aqueous interface as long as low potential scan rates ($v < 20$ mV s^{-1}) are used. The minor influence of the iR drop is due to the low currents, in the nanoampere range, associated with ion transfer across the μITIES arrays.

As noted previously [15, 21, 29], amperometric sensors are more suitable for incorporation into FIA systems than potentiometric sensors. Amperometric sensors have the ability to alter the selectivity of ion – transfer across the interface by controlling the Galvani potential difference ($\Delta_O^W\varphi = \varphi^W - \varphi^O$) using a potentiostat. Essentially, this allows selective transfer (or extraction) of ions from one phase to the other by applying a potential that corresponds to the characteristic Gibbs energy of transfer for that particular species. Thus, in this manner, a mixture of ions in solution may be selectively detected or separated. In contrast, potentiometric sensors lack the same degree of discrimination.

The potential window at the ITIES is limited by the Gibbs energy of transfer of the aqueous and organic phase electrolyte salts. Using an approach pioneered by Koryta [35], incorporation of ionophores into the organic phase allows detection of analyte ions (by lowering their Gibbs energy of transfer on binding with the ionophore) that would otherwise be incapable of transferring within the available potential window.

In this paper, we present the characterization of microfabricated silicon micropore arrays via voltammetry and amperometry under hydrodynamic conditions by their incorporation into a poly(tetrafluoroethylene) (PTFE) flow cell. Cyclic voltammetry of the direct ion transfer of positively and negatively charged model analytes under flowing

conditions reveals the different diffusion regimes (radial and linear) on either side of the μITIES. Flow rate studies in the presence of tetraethylammonium chloride (TEA^+) at the μITIES are carried out. The ability to construct hydrodynamic voltammograms of two oligopeptides, Phenylalanine dipeptide (Phe-Phe) and Lysine dipeptide (Lys-Lys), at the μITIES by the incorporation of an ionophore (dibenzo-18-crown-6 (DB18C6) ether) into the organogel and controlling the applied potential at the μITIES is presented.

2. Experimental

2.1. Reagents

All reagents were purchased from Sigma-Aldrich Ireland Ltd. and used without further purification, with the exception of 1,6-dichlorohexane (1,6-DCH) which was purified according to the published procedure [3]. The aqueous phase electrolytes of 10 mM LiCl and 10 mM HCl were prepared in ultrapure water (with a resistivity of 18 MΩ cm) from an Elgastat maxima – HPLC (Elga, UK). The model analyte species studied, i.e. the sodium salt of 4-octylbenzenesulfonate ($4\text{-}OBSA^-$) and the chloride salt of tetraethylammonium (TEA^+), were prepared in 10 mM LiCl aqueous phase. The oligopeptides studied were dilysine (Lys-Lys) and diphenylalanine (Phe-Phe). The oligopeptides were prepared in an aqueous electrolyte solution of 10 mM HCl, a pH at which they are positively charged. The ionophore used to facilitate the transfer of the oligopeptides was dibenzo-18-crown-6 ether (DB18C6). The organic electrolyte salt was prepared by metathesis of bis-(triphenylphosphoranylidene) ammonium chloride ($BTPPA^+ Cl^-$) and potassium tetrakis(4-chlorophenyl)borate ($K^+ TPBCl^-$) to obtain BTPPATPBCl, following the published experimental procedure [18].

2.2. Apparatus

Voltammetric and amperometric experiments at the μITIES array were performed using a CH Instruments 620B potentiostat (Texas). The electrochemical cell used in these studies is fabricated from poly(tetrafluoroethylene) (PTFE) and is based on that employed by Berduque et al. [29, 31] to electrochemically modulate the liquid-liquid extraction of ions at a macroITIES. The present design, detailed in Figure 1a, incorporates a borosilicate glass cylinder (6 mm external diameter, 3 mm inner diameter) with the microporous silicon membrane sealed onto the lower orifice using silicone rubber (RS Components, stock number 555-588). This design allows the aqueous phase to flow under the organogel supported in the silicon microporous membrane. The cell consists of two pieces that are held together using Teflon nuts and bolts and an o-ring (Viton O-ring, 25 mm approximate internal diameter and 1.8mm of thickness) to prevent leakage of the aqueous phase. The aqueous phase electrodes consist of a platinum mesh counter electrode and a Ag | AgCl reference electrode. A Ag | AgCl electrode in the organic reference solution acts as both the organic reference electrode and the organic counter electrode. The Ag | AgCl electrodes were prepared by the potentiostatic oxidation of silver wires in a solution of 3 M KCl.

The aqueous phase was introduced into the Teflon cell by means of a syringe pump (KD Scientific KDS200 series syringe pump) with controllable flow rates. A six-port valve (C22-3186 valve, Carl Stuart Ltd.) was used to inject samples via a 100-μL injection loop.

2.3. Preparation of the Organogels

The necessity of an ionophore (DB18C6 ether) in the organic phase to facilitate the transfer of the oligopeptides across the ITIES required the preparation of two distinct organogels. The first organogel, detailed in cell 1 (Figure 1b), did not contain the ionophore and was used as the organic phase in the model analyte studies, while the second organogel, detailed in cell 2 (Figure 1b), contained the ionophore and was used in the oligopeptide

studies. The remaining components of the organogel consisted of an organic solvent (1,6-DCH), an organic electrolyte (BTPPATPBCl) and the low molecular weight polyvinylchloride (PVC). A detailed description of organogel preparation is given elsewhere [11].

2.4. Micropore array designs and fabrication

The micropore arrays were fabricated from 525 μm thick silicon wafers using a combination of wet and dry silicon etching to thin the wafers and etch pores through the thinned portions, as described elsewhere [9]. The fabrication procedure produced pores with hydrophobic walls, facilitating the filling of the pores with organic phase [9]. Two micropore array designs are used in the course of these studies. Design 1 consists of 23 micropores in a hexagonal close packed arrangement. Each individual pore measures 52 μm in diameter and the pore-to-pore (center-to-center) distance is 250 μm. Design 2 consists of 8 micropores in a hexagonal close packed arrangement. Each individual pore measures 52 μm in diameter and the pore-to-pore (center-to-center) distance is 500 μm. The organogel was inserted into the glass cylinder as a liquid at ~60°C using a glass pipet. In this manner the hydrophobic pores of the micropore array are completely filled rendering an inlaid interfacial geometry on the aqueous side of the ITIES [9, 11, 34].

2.5. Methodology

By convention [4], positive currents are caused by the transfer of cations from the aqueous phase (w) to the organic phase (o) (or by anions from o to w). On the contrary, negative currents arise as a result of anions transferring from w to o (or by the cations transferring from o to w). The pore-to-pore (center-to-center) spacing of both micropore array designs is sufficiently large (≥ 10 radius of the pore) to prevent interactions between the

individual diffusion fields. As a result steady – state voltammetric responses are expected on transfer of an analyte from w to o due to spherical diffusion at the mouth of the micropore. Conversely, peak – shaped responses are expected on transfer of an analyte from o to w due to the recessed geometry creating a linear diffusion field on the organic side of the ITIES [9].

Once the experimental setup is complete the electrochemical cell is filled with the desired aqueous phase by flowing the liquid at the relatively quick volumetric flow rate of 1 mL min^{-1} using the syringe pump. The cell can be deemed full once drops of aqueous phase begin to fill the waste receptacle placed under the exit tube. At this point the flow of the solution is halted, and a stationary cyclic voltammogram (CV) of the solution is run. In this manner the cell setup and parameters used can be verified prior to each experiment [29]. Thereafter, desired flow rates are set and aliquots of target analyte solutions injected into the flowing aqueous phase.

4. Results and Discussion

4.1. Model Ion studies: Cyclic Voltammetry

The CV responses of a positively (TEA^+) and a negatively (4-$OBSA^-$) charged analyte species at the μITIES array under flowing conditions were investigated. Electrochemical cell 1 (Figure 1b) and micropore array design 1 (see experimental section) were utilized for the study of the model ions. In cell 1 the identity of the target analyte species (either TEA^+ or 4-$OBSA^-$) is represented by **a**, and **j** represents the species molar concentration.

The CV response of 4-$OBSA^-$ under flowing conditions is illustrated in Figure 2a. The flowing aqueous phase contained an injected aliquot of 0.5 mM 4-$OBSA^-$ in background electrolyte. The volumetric flow rate used was 1 mL min^{-1} and the CV scan rate was 5 mV s^{-1}. The negative sweep (the forward sweep in this case) was found to be sigmoidal in shape and the positive sweep (the reverse sweep in this case) was found to be peak shaped.

Theoretically, the anionic 4-OBSA$^-$ should yield a negative CV response on transferring from w to o. In addition, since the geometry of the micropore is inlaid on the aqueous side of the interface the negative response should be sigmoidal in shape, as observed in Figure 2a. Conversely, a positive CV response is expected on 4-OBSA$^-$ transferring from o to w, and due to the recessed geometry on the organic side of the interface a peak shaped response is anticipated, also as observed in Figure 2a.

The CV response of TEA$^+$ under flowing conditions is expected to give the opposite response to 4-OBSA$^-$, as illustrated in Figure 2b. The flowing aqueous phase contained and aliquot of 0.1 mM TEA$^+$ in background electrolyte. The volumetric flow rate used was 0.25 mL min^{-1} and the CV scan rate was 5 mVs^{-1}. The positive sweep (the forward sweep in this case) was found to be sigmoidal in shape, due to the transfer of a cationic species from w to 0, and the negative sweep (the reverse sweep in this case) was found to be peak shaped, due to the transfer of a cationic species from o to w.

4.2. Model Ion Studies: Influence of Flow Rate on Amperometric Response

The variation of the amperometric response of TEA$^+$ with flow rate at the μITIES array was investigated. The cell was filled with the aqueous phase (10 mM LiCl) and a stationary CV of the blank attained, as described in the methodology. Berduque et al. [29, 31] have shown that the magnitude of the TEA$^+$ transfer peak depends on the applied potential ($\Delta_O^W\phi$). A cationic species will transfer from w to o on the application of a potential positive of the analyte's formal transfer potential. Thus, the potential was set to the sufficiently positive value, using amperometry, of 0.9 V so as to ensure a maximum rate at which TEA$^+$ can be extracted into the organogel. The flow in the cell was set at the particular flow rate to be studied, one of 0.05, 0.15, 0.25, 0.35, 0.5, 0.65, 0.8 or 1.00 mL min^{-1}, and the background current allowed to stabilize. Subsequently an injection of 1 mM TEA$^+$ in 10 mM LiCl was

performed using the 100 μL volume sample loop and the amperometric response recorded. Figure 3 shows the reproducibility attained at different flow rates tested. The percentage relative standard deviations (RSD), over 3 sample injections, at all flow rates varied in the range 2 – 4 %.

For the current at interfaces embedded in a flow channel two limiting behaviours can be encountered, corresponding to the limiting cases of diffusion or convection dominating the mass transport. When convection dominates, the steady state current follows the well known Levich equation [36], with the steady state current proportional to $v_{av}^{1/3}$, where v_{av} is the average flow velocity of the liquid along the length of the channel. On the contrary, when diffusion is the main transport mode, the limiting current is not expected to show a dependence on the flow velocity. Figure 4a indicates diffusion dominated mass transport, since the height of the current does not increase with the cube root of the volumetric flow, but remains constant. This behaviour can be explained in terms of diffusion and hydrodynamic layers, where the (steady-state) diffusion layer thickness perpendicular to the micropores does not exceed the thickness of the hydrodynamic layer for any volumetric flow rate used in this study. A qualitative description of this behaviour is illustrated by the concentration profile shown in Figure 5, where the extension of the diffusion layer has been approximated by the Nernst layer thickness, δ_N, and δ_{Ha} and δ_{Hb} represent the thickness of hydrodynamic layers of lower (δ_{Hb}) and higher (δ_{Ha}) flow rates.

The dependence of the half peak width of the current-time peaks and of the charge flow on the volumetric flow rate is shown in Figure 4(b) and 4(c). With decreasing flow rate, both the half peak width and the charge increase. This is explained by the increased time period the μITIES are in contact with the analyte with decreasing volumetric flow rates. Consequently, at lower flow rates, the ion transfer can take place over a longer time and more ions (charge) can be transferred across the interfaces.

4.3. Analysis of Oligopeptides: Cyclic Voltammetry

CV responses of the positively charged oligopeptides Phe-Phe and Lys-Lys at the μITIES array under stationary conditions were initially investigated, as illustrated in Figure 6. Electrochemical cell 2 (Figure 1b) and micropore array design 2 (see experimental section) were utilized for the study of the oligopeptides. In cell 2 the identity of the target oligopeptide is represented by **b**, and **j** represents the species molar concentration. Once the electrochemical cell was filled with the aqueous phase (0.2 mM of either Phe-Phe or Lys-Lys in 10 mM HCl) the flow was halted and a stationary CV carried out, as described in the methodology. Based on the properties of the individual oligopeptides at pH 2 (ionic charge, hydrophilicity, ability of the side chain to complex the crown ether DB18C6), as described in detail previously [11], one would expect Phe-Phe to transfer at a lower potential than Lys-Lys, and that Lys-Lys would produce the greater transfer peak currents. The expected trends were indeed observed (Figure 6) and the CVs act as a good indicator of the applied potentials necessary to electrochemically modulate the transfer from w to o of either oligopeptide in subsequent FIA studies. Finally, the expected steady – state signal on transfer from w to o was observed for Phe-Phe but not Lys-Lys. This may be due to the forward transfer peak of Lys-Lys being masked by the background electrolyte transfer at higher potentials or simply the steady – state response may occur outside the available potential window. Both oligopeptides generated the expected peak shaped responses for the reverse, o to w, transfer process.

4.4. Analysis of Oligopeptides: Influence of Applied Potential on Amperometric Response

The influence of the applied potential ($\Delta_O^W\phi$) on the amperometric response of both Phe-Phe and Lys-Lys at the μITIES array was investigated. The cell was filled with the aqueous phase (10 mM HCl) and a stationary CV of the blank attained, as described in the

methodology. The potential was set to a specific value (in the studied range 0.3 – 0.75 V) and the flow was initiated at a volumetric flow rate of 0.5 mL min^{-1}. On stabilization of the background current a 100 μL injection of either 1 mM Phe-Phe or Lys-Lys in 10 mM HCl was carried out. For both oligopeptides, multiple sample injections (n = 3) at each applied potential were performed.

Analogous to previous potentiostatic extraction studies on cations at a macroITIES [29, 31], on injection of Phe-Phe or Lys-Lys into the flow cell positive current peaks were observed, indicative of the transfer of a cation from w to o. Figure 7 is representative of typical peak current responses of an oligopeptide at different applied potentials, in this case Phe-Phe. The time axis is normalized with respect to the time at which the sample injections were made. The magnitude of these peaks was dependent on the applied potential across the interface. The percentage relative standard deviations (RSD), over 3 sample injections for the applied potentials studied, varied in the range 2 – 10 % with both oligopeptides.

At $\Delta_O^W\phi \geq 0.675$ V for Phe-Phe and $\Delta_O^W\phi \geq 0.725$ V for Lys-Lys, the amperometric peak current stabilizes and reached a plateau. CV analysis in Figure 6 revealed that the steady – state conditions had been attained for Phe-Phe by 0.675 V and the maximum current reached by Lys-Lys occurred at the upper limits of the available potential window. Therefore, the applied potential – independent currents are indicative of the maximum rate of transfer for the particular oligopeptides into the organogel.

4.5. Analysis of Oligopeptides: Hydrodynamic Voltammograms

Hydrodynamic Voltammograms (HDVs) are constructed by plotting the average amperometric peak currents at each applied potential for a given transferring species versus the applied potential ($\Delta_O^W\phi$). HDV curves for Phe-Phe and Lys-Lys are illustrated in figure 8. HDV curves are of particular benefit when carrying out a comparative study into the

magnitude of the applied potential necessary to electrochemically transfer (or extract) an analyte from one phase to another. If these analytes are in a mixture they may be selectively extracted or co-extracted depending on the applied potential.

Berduque et al. [29, 31] have established that for cationic species increased levels of transfer from w to o occur moving to more positive potentials, eventually reaching a maximum at $\Delta_O^W\phi \geq$ the peak potential of the ion. For anionic species the opposite is true with the maximum rate of extraction observed at values of $\Delta_O^W\phi \leq$ the peak potential of the ion. A hydrodynamic voltammogram for a specific analyte can be broken down into 3 distinct regions: (1) a range of applied potentials over which no amperometric peaks are observed, (2) a range of applied potentials where successively higher peak currents are observed and (3) a range of applied potentials where potential – independent behavior of the amperometric peak current is observed. In agreement with the CV data in Figure 6, the electrochemically modulated transfer of Phe-Phe is seen to begin at lower applied potentials than is the case for Lys-Lys. The magnitude of the maximum Phe-Phe peak current response is less than that of Lys-Lys, and the maximum rate of transfer is also attained at a lower applied potential for Phe-Phe. Based on the HDV results in Figure 8 selective extraction of Phe-Phe from Lys-Lys would be possible at an applied potential of ~0.525 V.

5. Conclusions

Micrometre-sized ITIES arrays incorporated into a flow cell were characterized via cyclic voltammetry with model analyte species. It was found that the interface was inlaid on the aqueous side of the microporous silicon membrane used to define the array and recessed on the organic side, based on the CV shapes obtained for model analytes and the diffusion profiles that define these shapes. The current at the electrodes embedded in the flow channel is limited by diffusion-dominated mass transport, as indicated by the independence of the

steady – state current from the flow velocity of the aqueous phase. This behavior is due to the fact that the steady – state diffusion layer thickness perpendicular to the microinterfaces does not exceed the thickness of the hydrodynamic layer for any volumetric flow rate employed. The incorporation of the ionophore DB18C6 into the organogel facilitated the transfer of oligopeptides (Phe-Phe and Lys-Lys) across the μITIES array under flowing conditions. Each individual oligopeptide has a characteristic Gibbs energy of transfer based on an interplay of factors such as charge, hydrophobicity and the ability of the oligopeptide to interact with the ionophore. The magnitude of the amperometric peak currents for each oligopeptide were shown to be dependent on the applied potential ($\Delta_O^W\phi$) and hydrodynamic voltammograms constructed from the amperometric peak currents at each applied potential show that Phe-Phe may be selectively extracted from a mixture containing Lys-Lys at $\Delta_O^W\phi \approx 0.525$ V. These data demonstrate that hydrodynamic μITIES arrays engineered within microporous silicon membranes may be usefully employed as detectors for flow analytical methods such as liquid chromatography, capillary electrophoresis or flow-injection analysis.

Acknowledgements

This work was supported by Science Foundation Ireland (Grants 02/IN.1/B84 and 07/IN.1/B967), the Irish Research Council for Science, Engineering and Technology (Embark Postgraduate Research Scholarship Scheme Grant RS/2005/122 (to M.D.S.)) and the European Commission, Marie Curie Transfer of Knowledge Programme (Grant MTKD-CT-2005-029568 (to J. S)).

Figure Captions

Figure 1: (a) Schematic diagram of the PTFE microscaled electrochemical cell. (X) Organic phase Ag / AgCl reference electrode. (X) also acts as the organic phase counter electrode. (Y) Aqueous phase Ag / AgCl reference electrode. (Z) Platinum mesh counter electrode for the aqueous phase. (b) Electrochemical cell configurations utilized in this study.

Figure 2: Cyclic voltammetry of model ions in a flowing aqueous phase at the μITIES. (a) CV response of 0.5 mM 4 – $OBSA^-$ (in 10 mM LiCl flowing aqueous phase) across the μITIES. Flow rate: 1 mL min^{-1}. Scan rate: 5 mVs^{-1}. (b) CV response of 0.1 mM TEA^+ (in 10 mM LiCl flowing aqueous phase) across the μITIES. Flow rate: 0.25 mL min^{-1}. Scan rate: 5 mVs^{-1}. The transfer potentials are relative to the Ag / AgCl reference electrodes used.

Figure 3: Amperometric response of TEA^+ vs flow rate. Applied potential ($\Delta_O^W\phi$) = 0.9 V. Sample injection of 100 μL of 1 mM TEA^+ in 10 mM LiCl. Three sample injections per flow rate test.

Figure 4: (a) Variation of TEA^+ amperometric peak current with the cube root of the flow rate. (b) Variation of the charge and (c) the half peak width (HPW) of the TEA^+ amperometric peak with flow rate. Error bars indicate the standard deviation of the triplicate measurements.

Figure 5: Theoretical concentration profile of TEA^+ transfer at varying flow rates. C_o^* = concentration of TEA^+ in the bulk aqueous solution, δ_N = Nernst Diffusion Layer, δ_{Ha} = Hydrodynamic Boundary Layer at fast flow rates, δ_{Hb} = Hydrodynamic Boundary Layer at slow flow rates.

Figure 6: Cyclic voltammetry of oligopeptides in a stationary aqueous phase at the μITIES. CV response of (a) blank (black), (b) 0.2 mM Phe – Phe (blue) and (c) 0.2 mM Lys – Lys (red). Scan rate: 10 mVs^{-1}. The transfer potentials are relative to the Ag / AgCl reference electrodes used.

Figure 7: Amperometric response of Phe – Phe as a function of the applied potential ($\Delta_O^W\phi$). The applied potentials were, in the order of increasing peak height, 0.6 (light grey), 0.625, 0.65, 0.665, 0.675 and 0.7 (black) V. The amperometric peak currents were normalized with respect to the time at which each injection was performed. Flow rate: 0.5 mL min^{-1}. Sample injection of 100 μL of 1 mM Phe – Phe in 10 mM HCl. Three sample injections per applied potential ($\Delta_O^W\phi$).

Figure 8: Hydrodynamic voltammograms for Phe – Phe (blue circles) and Lys – Lys (red diamonds). Flow rate: 0.5 mL min^{-1}. Sample injection of 100 μL of either 1 mM Phe – Phe or 1 mM Lys – Lys in 10 mM HCl. Three sample injections per applied potential ($\Delta_O^W\phi$).

Figure 1 (a)

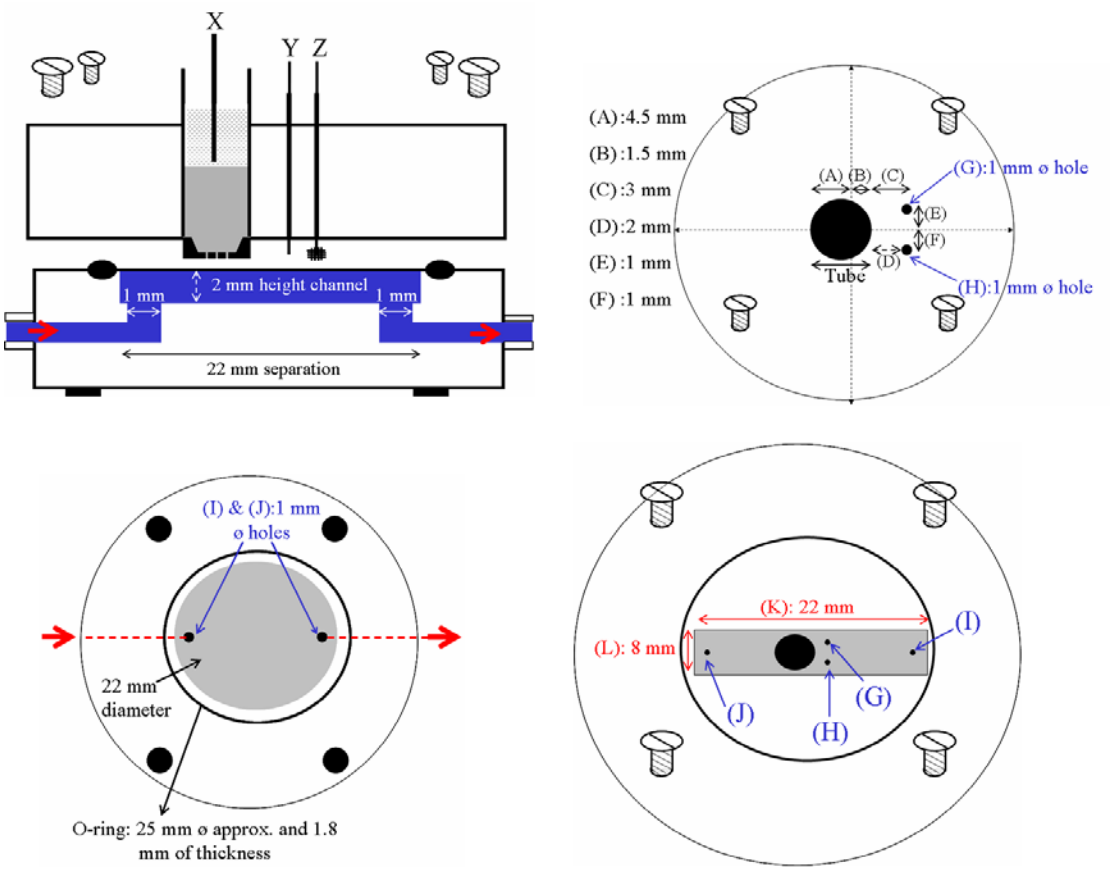

Figure 1 (b)

Cell 1:

$Ag_{(s)}$	$AgCl_{(s)}$	10 mM BTPPACl 10 mM LiCl (aq.)	10 mM BTPPATPBCl Gellified 1,6-DCH	$\mathbf{a}_j$ mM in 10 mM LiCl (aq.)	$AgCl_{(s)}$	$Ag_{(s)}$

Cell 2:

$Ag_{(s)}$	$AgCl_{(s)}$	10 mM BTPPACl 10 mM LiCl (aq.)	10 mM BTPPATPBCl 10 mM DB18C6 Gellified 1,6-DCH	$\mathbf{b}_j$ mM in 10 mM HCl (aq.)	$AgCl_{(s)}$	$Ag_{(s)}$

Figure 2 (a)

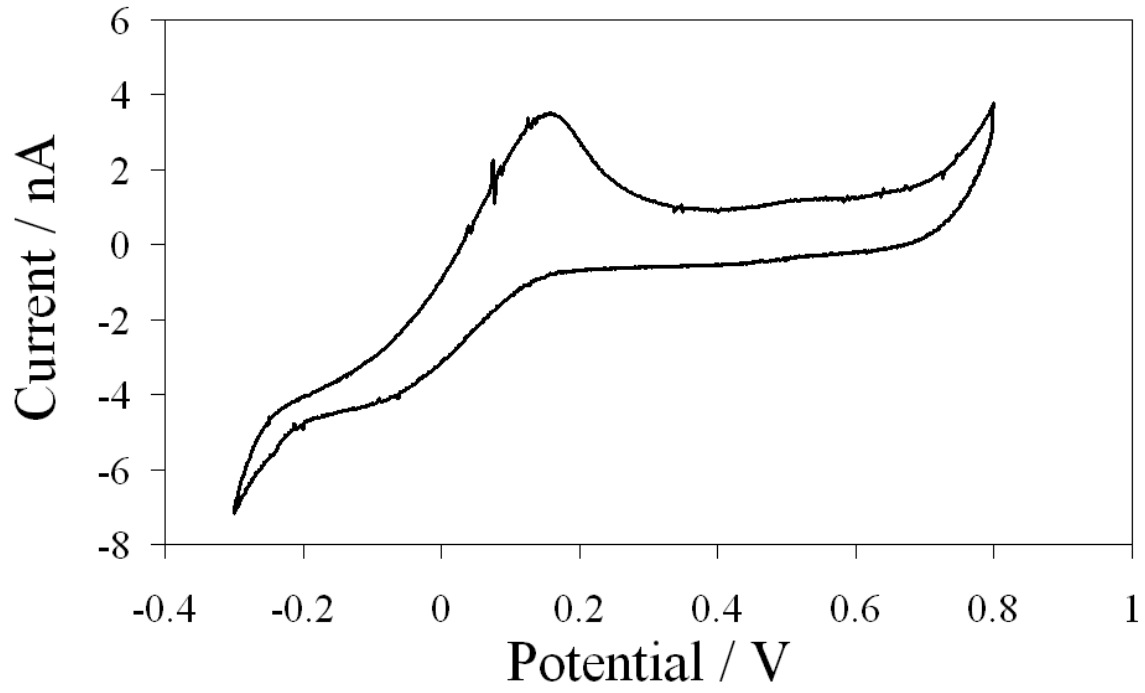

Figure 2 (b)

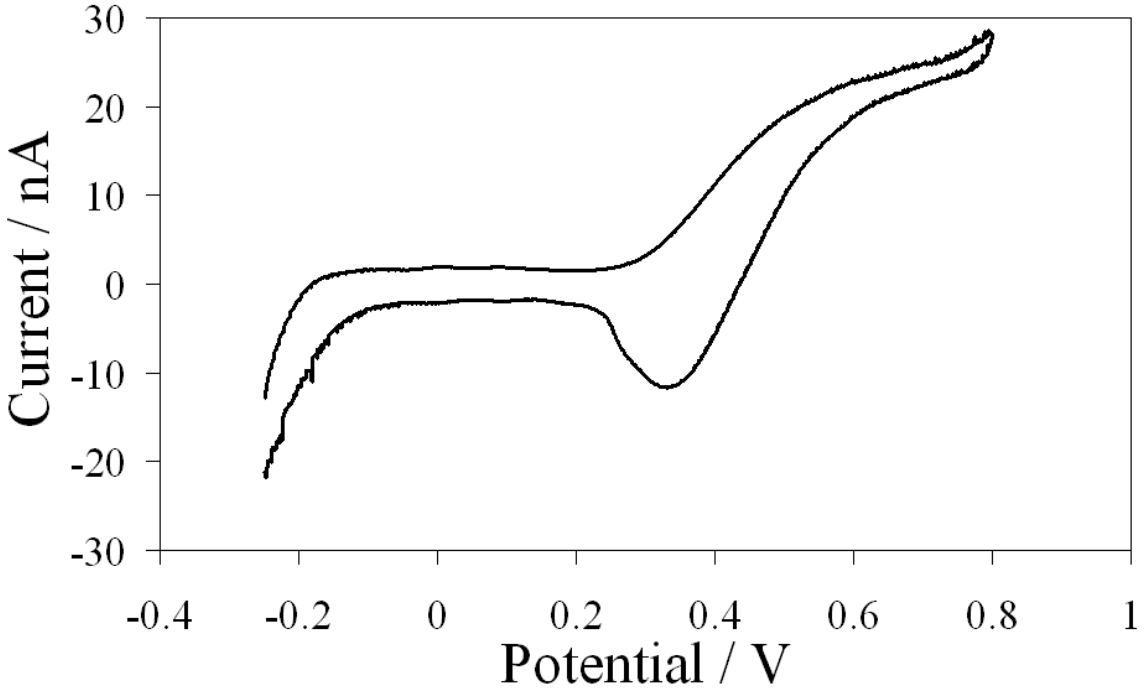

Figure 3

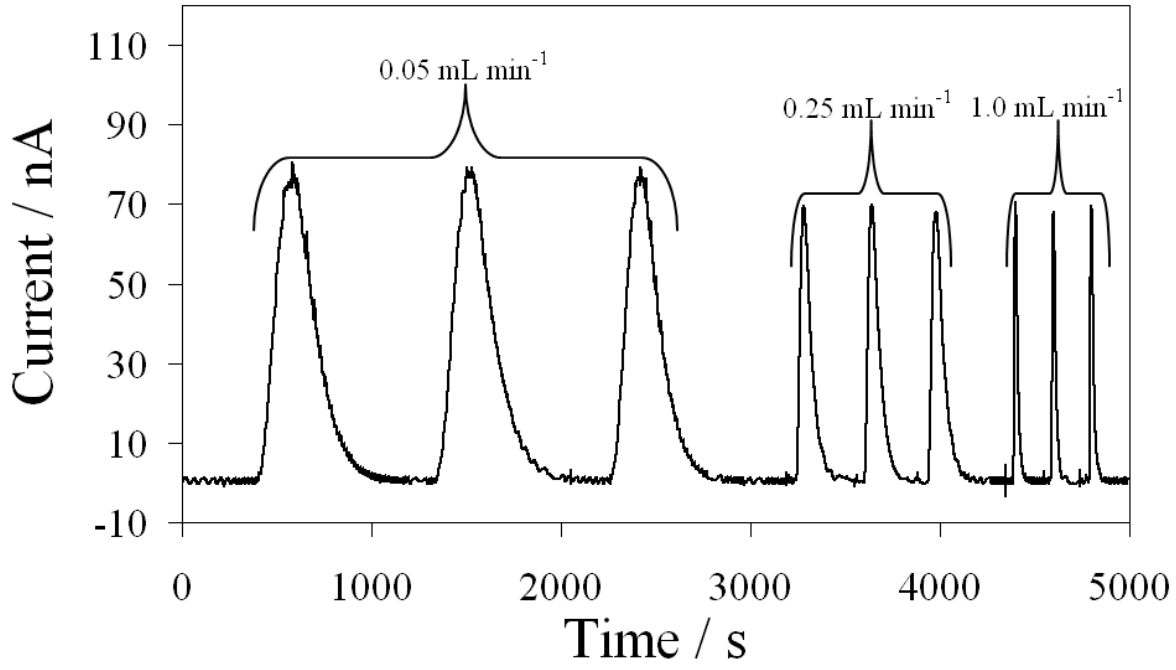
0.05 mL min-1
0.25 mL min-1
1.0 mL min-1
Current / nA
110
90
70
50
30
10
-10
0
1000
2000
3000
4000
5000
Time / s

Figure 4 (a)

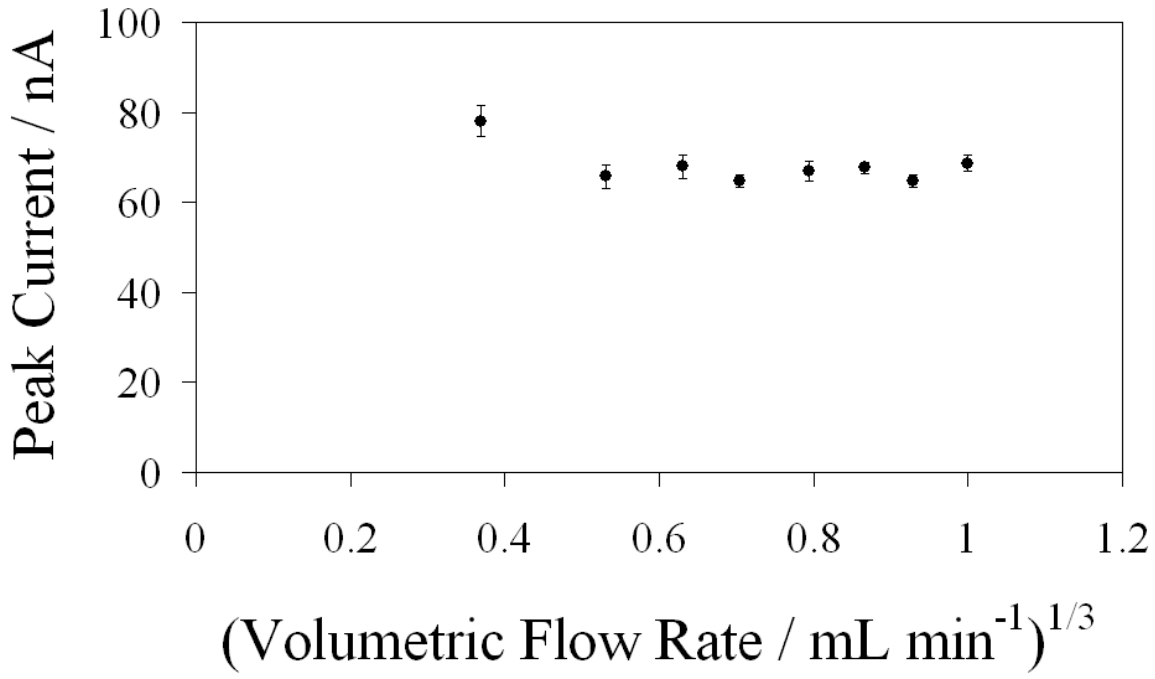

Figure 4 (b)

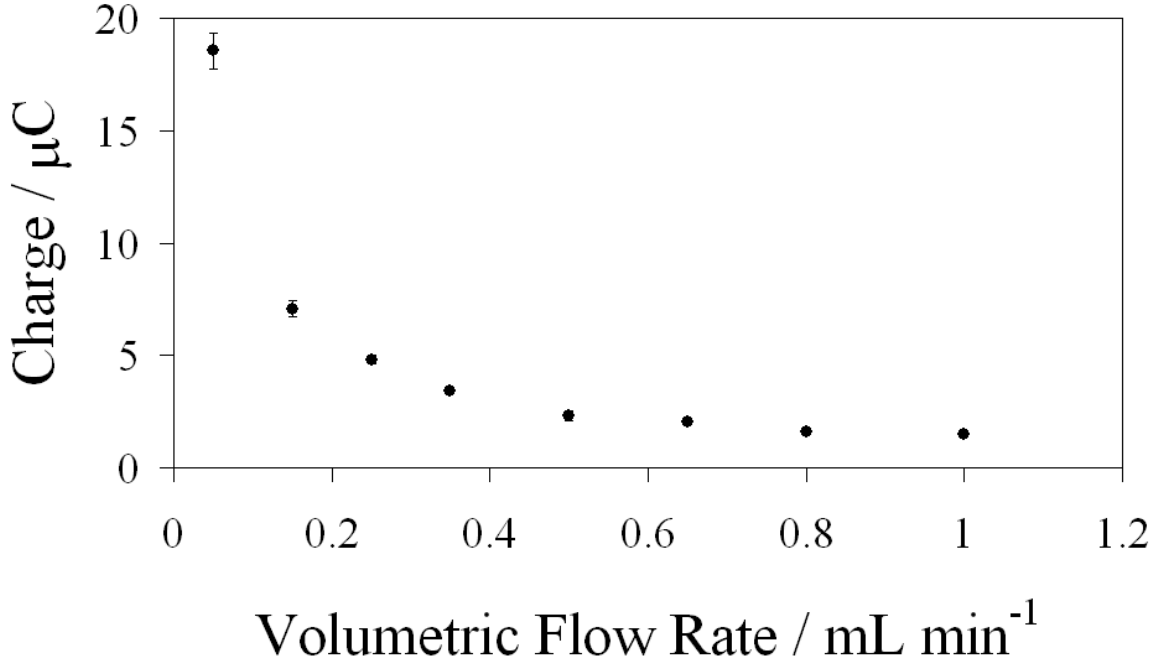

Figure 4 (c)

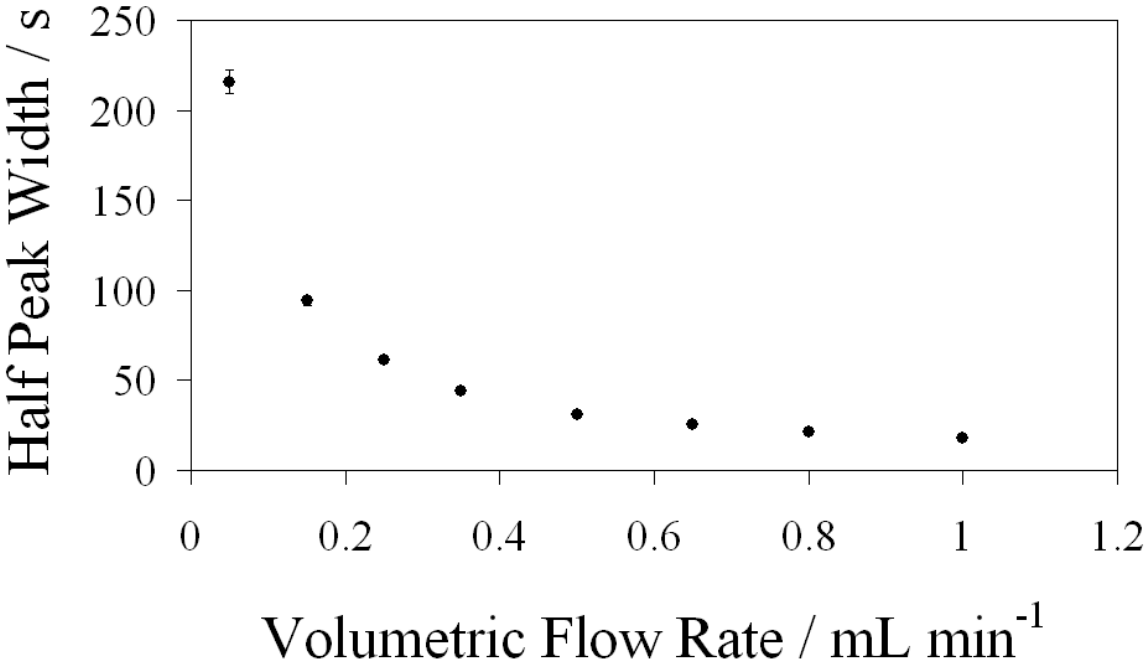
Half Peak Width / s
250
200
150
100
50
0
0
0.2
0.4
0.6
0.8
1
1.2
Volumetric Flow Rate / mL min-1

Figure 5

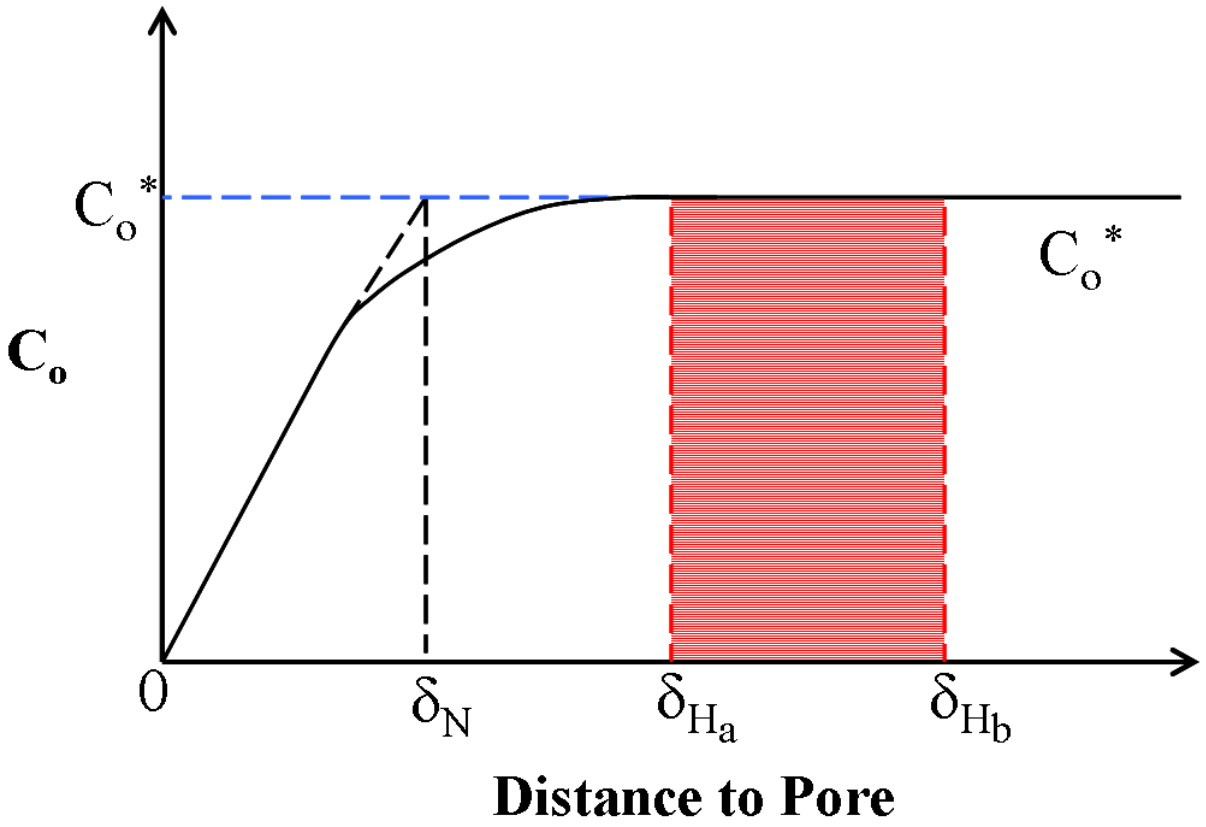

Figure 6

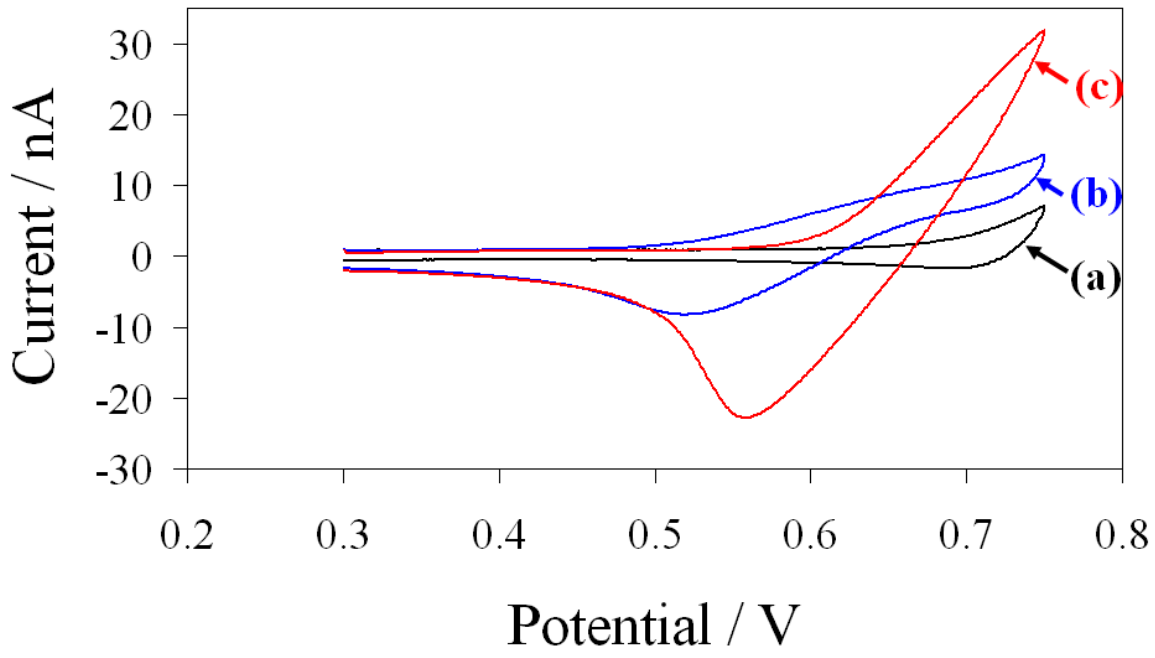

Figure 7

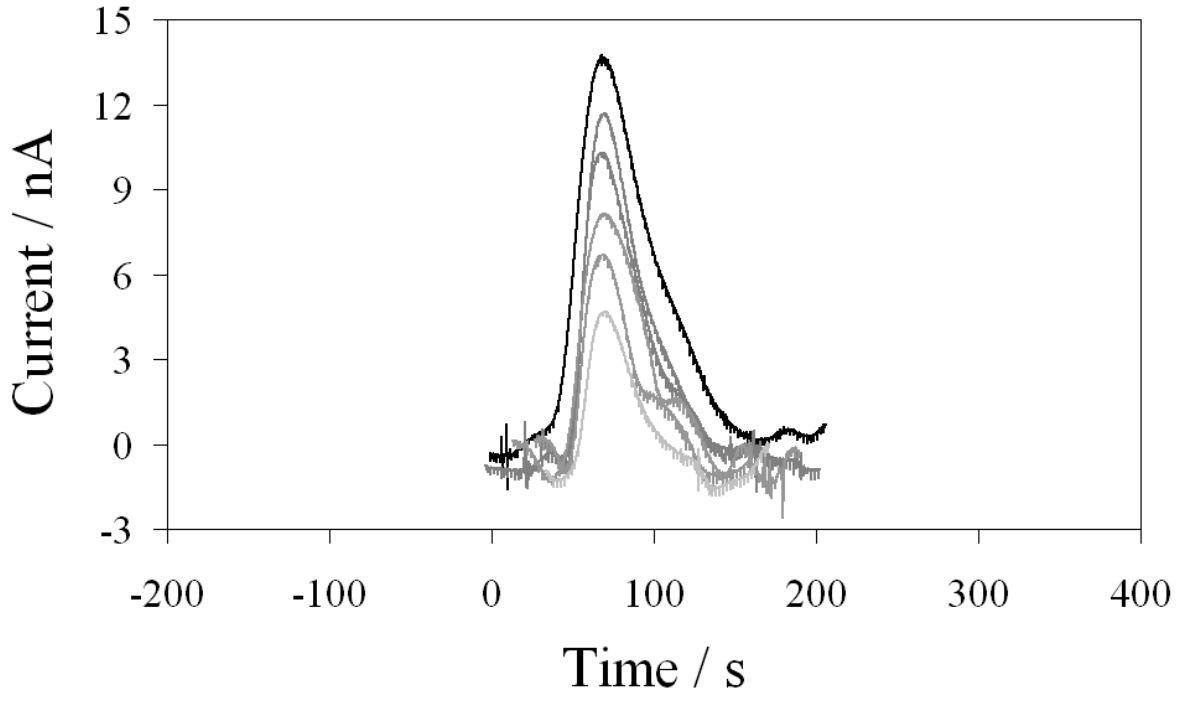

Figure 8

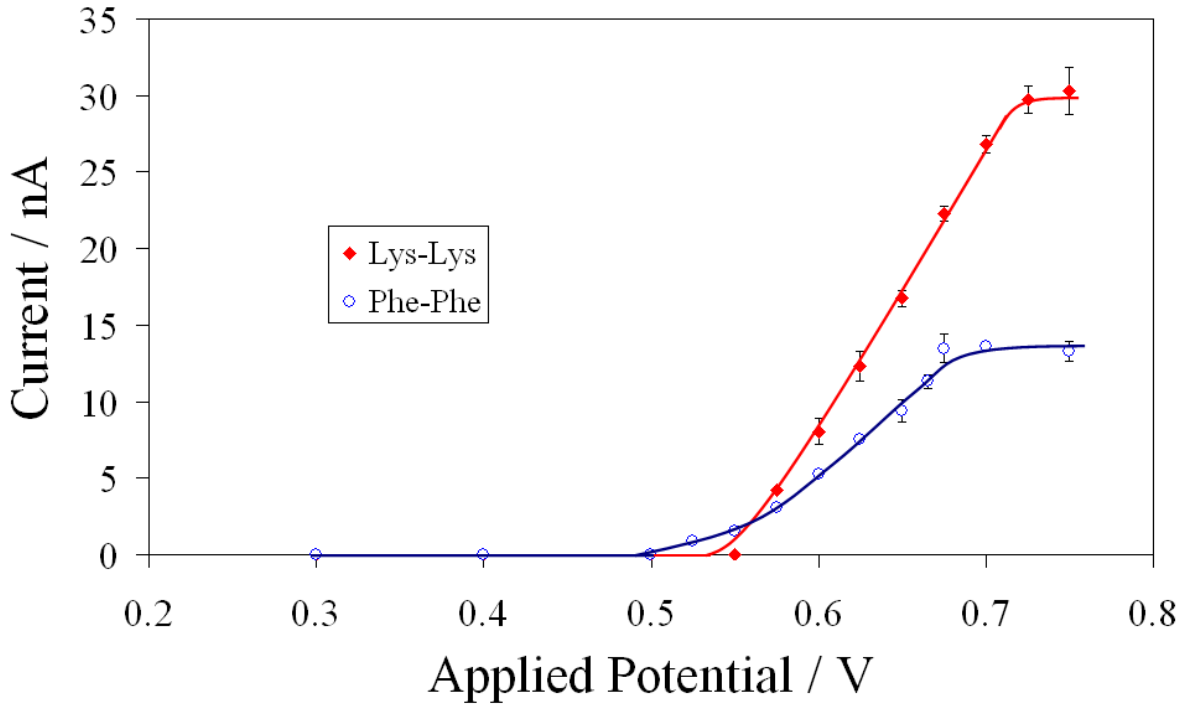
35
30
25
20
15
10
5
0
Current / nA
Lys-Lys
Phe-Phe
0.2
0.3
0.4
0.5
0.6
0.7
0.8
Applied Potential / V

References

[1] A. Sherburn, M. Platt, D.W.M. Arrigan, N.M. Boag, R.A.W. Dryfe, Analyst, 128 (2003) 1187.
[2] D.W.M. Arrigan, M. Ghita, V. Beni, Chem. Commun., (2004) 732.
[3] H. Katano, H. Tatsumi, M. Senda, Talanta, 63 (2004) 185.
[4] Z. Samec, Pure Appl. Chem., 76 (2004) 2147.
[5] Z. Samec, E. Samcová, H.H. Girault, Talanta, 63 (2004) 21.
[6] V. Beni, M. Ghita, D.W.M. Arrigan, Biosens. Bioelectron., 20 (2005) 2097.
[7] A.M. O'Mahony, M.D. Scanlon, A. Berduque, V. Beni, D.W.M. Arrigan, E. Faggi, A. Bencini, Electrochem. Commun., 7 (2005) 976.
[8] A. Berduque, M.D. Scanlon, C.J. Collins, D.W.M. Arrigan, Langmuir, 23 (2007) 7356.
[9] R. Zazpe, C. Hibert, J. O'Brien, Y.H. Lanyon, D.W.M. Arrigan, Lab Chip, 7 (2007) 1732.
[10] G. Herzog, V. Kam, A. Berduque, D.W.M. Arrigan, J. Agric. Food Chem., 56 (2008) 4304.
[11] M.D. Scanlon, G. Herzog, D.W.M. Arrigan, Anal. Chem., 80 (2008) 5743.
[12] V. Marecek, H. Jänchenová, M.P. Colombini, P. Papoff, J. Electroanal. Chem., 217 (1987) 213.
[13] B. Hundhammer, S. Wilke, J. Electroanal. Chem., 266 (1989) 133.
[14] E. Wang, H. Ji, Electroanalysis, 1 (1989) 75.
[15] S. Wilke, H. Franzke, H. Müller, Anal. Chim. Acta, 268 (1992) 285.
[16] B. Hundhammer, T. Solomon, T. Zerihun, M. Abegaz, A. Bekele, M. Graichen, J. Electroanal. Chem., 371 (1994) 1.
[17] S. Wilke, Anal. Chim. Acta, 295 (1994) 165.
[18] H.J. Lee, P.D. Beattie, B.J. Seddon, M.D. Osborne, H.H. Girault, J. Electroanal. Chem., 440 (1997) 73.
[19] H.J. Lee, C. Beriet, H.H. Girault, J. Electroanal. Chem., 453 (1998) 211.
[20] H.J. Lee, H.H. Girault, Anal. Chem., 70 (1998) 4280.
[21] S. Sawada, H. Torii, T. Osakai, T. Kimoto, Anal. Chem., 70 (1998) 4290.
[22] H.J. Lee, C.M. Pereira, A.F. Silva, H.H. Girault, Anal. Chem., 72 (2000) 5562.
[23] S. Wilke, R. Schurz, H. Wang, Anal. Chem., 73 (2001) 1146.
[24] C. Sánchez-Pedreño, J.A. Ortuño, J. Hernández, Anal. Chim. Acta, 459 (2002) 11.
[25] S. Sawada, M. Taguma, T. Kimoto, H. Hotta, T. Osakai, Anal. Chem., 74 (2002) 1177.
[26] S.S. Hill, R.A.W. Dryfe, E.P.L. Roberts, A.C. Fisher, K. Yunus, Anal. Chem., 75 (2003) 486.
[27] B. Kralj, R.A.W. Dryfe, J. Electroanal. Chem., 560 (2003) 127.
[28] J.A. Ortuño, J. Hernández, C. Sánchez-Pedreño, Electroanalysis, 16 (2004) 827.
[29] A. Berduque, A. Sherburn, M. Ghita, R.A.W. Dryfe, D.W.M. Arrigan, Anal. Chem., 77 (2005) 7310.
[30] J.A. Ortuño, C. Sánchez-Pedreño, A. Gil, Anal. Chim. Acta, 554 (2005) 172.
[31] A. Berduque, D.W.M. Arrigan, Anal. Chem., 78 (2006) 2717.
[32] J.A. Ortuño, A. Gil, C. Sánchez-Pedreño, Sens. Actuators B, 122 (2007) 369.
[33] J.A. Ortuño, A. Gil, C. Serna, A. Molina, J. Electroanal. Chem., 605 (2007) 157.
[34] J. Strutwolf, M.D. Scanlon, D.W.M. Arrigan, Analyst, (2009) DOI: 10.1039/b81526j.
[35] J. Koryta, Electrochim. Acta, 24 (1979) 293.
[36] V.G. Levich, Physicochemical Hydrodynamics, Prentice Hall, New Jersey, 1962.